E-ISSN: 2664-6773
P-ISSN: 2664-6765
Impact Factor: RJIF 5.6
IJCBS 2024; 6(1): 139-145
www.chemicaljournal.org
Received: 18-02-2024
Accepted: 24-03-2024

Thaaer Khalil
Department of Chemistry, College of Science, Tikrit University, Tikrit, Iraq

Khalaf A Jasim
Department of Chemistry, College of Science, Tikrit University, Tikrit, Iraq

Ahmed S Faihan
Department of Chemistry, College of Science, Tikrit University, Tikrit, Iraq

Reza Behjatmanesh-Ardakani
Department of Chemical Engineering, Faculty of Engineering, Ardakan University, P.O. Box 184, Ardakan, Iran

Corresponding Author:
Ahmed S Faihan
Department of Chemistry, College of Science, Tikrit University, Tikrit, Iraq

Synthesis, characterization and theoritical study of some pyrazine carbohydrazide derivatives

Thaaer Khalil, Khalaf A Jasim, Ahmed S Faihan and Reza Behjatmanesh-Ardakani

DOI: https://doi.org/10.33545/26646765.2024.v6.i1b.117

Abstract
In the current work, we report the synthesis and characterization of some pyrazine carbohydrazide derivatives; namely: N'-(2-hydroxybenzylidene) pyrazine-2-carbohydrazide (Hmbpcz), N'-(2-hydroxy-4-methoxybenzylidene) pyrazine-2-carbohydrazide (Hbpcz), and N'-(2-hydroxy-4-methoxybenzylidene) benzohydrazide (Mbbz). The procedure includes the reaction of 4-methoxy salicaldehyde and pyrazine carbohydrazide in a 1:1 molar ratio. The synthesized compounds were confirmed by NMR and IR. Moreover, the three compounds were theoretically investigated using the Density Functional Theory (DFT) approach with the B3LYP/Def2-TZVP basis set. Each of the three compounds exhibited a planar structure characterised by a strong π-electron resonance across the entire molecule. Among the compounds, compound Mbbz exhibited the greatest HOMO-LUMO energy gap, whilst compound Hmbpcz obtained the lowest. Moreover, the calculations of the natural bond orbital (NBO) revealed that the pyrazine ring surpasses the benzene ring in its ability to transfer electrons to the pi system. The stability values of all compounds were greatly enhanced by the presence of π-electron resonance in the ligands.

Keywords: Pyrazine carbohydrazide, schiff base, DFT, hydazones, hydrazides

Introduction
Hydazones are chemical compounds including oxygen and nitrogen atoms. Various applications of hydroxyzone derivatives have been extensively documented in literature, particularly as highly promising antifungal agents [1-4]. Their distinctive capacity to form coordination complexes with various transition metals via their N-heterocyclic or O-phenolic atoms, carbonyl group, and azomethane group derivatives has established them as significant ligands in coordination chemistry [5-8]. For instance, Choudhary and Morrow have reported a series of mixed ligand acylhdrazone complexes with interesting geometries [9]. Moreover, compounds containing hydrazides have demonstrated remarkable biological activity. The recent endeavours to address the problem of multiresistant bacterial strains have shifted the attention towards exploring different strategies, such as the alteration of the structure of current medications. For instance, Backes at. el al., has reported a series of phenylhydrazones of 5-acylpyrimidinetrione [10]. These drugs have demonstrated strong growth suppression with low cell toxicity when used against two human pathogenic species, Candida albicans and Candida glabrata. Moreover, salicylaldehyde hydrazone derivatives have been shown to possess antibacterial properties, although salicyladehydes lack such activity [11-13]. Pyrazinamide and pyrzanoic acid are primary medicinal drugs used in the treatment of tuberculosis infections [14]. The Surface Activation Reactivity (SAR) of pyrzinamide derivatives is much restricted because they are exclusively used in acidic environments. The proposed approach involves the integration of two distinct pharmacophore units inside a single frame to generate hybrid compounds. Thus, Pyrzaine carbohydrazide can be employed for the synthesis of novel derivatives of Schiff base hydrazide, which is theoretically expected to enhance their biology. Pyrzanoic acid can serve as a precursor for esterification to produce methyl-pyrainoate, which, when combined with hydrazine hydrate, forms pyrazine carbohydrazide. Various Schiff base derivatives of pyrazine carbohydrazide are formed by reacting the latter with different aldehyde moieties.

Experimental Section
Synthesis of the carbohydrazide derivatives
Pyrazine carbohydrazide: Pyrazine-2-carboxylic acid (0.01 mole, 1.24 g) was dissolved in

methanol (50 mL) with few drops of conc. Sulfuric acid which was refluxed for 72 h; Next NH_2NH_2 (100%) (0.3 mol) was added and the mixture was allowed to reflex for 8hrs. The mixture was allowed to slowly evaporate which results in an orange crystal of the targeted compound. The crystals were filtered off, washed with cold ethanol and vacuum dried (81%, yield, m.p. 170 °C).

General procedure for the synthesis of acid hydrazide Schiff Bases: To a stirred solution of Pyrazine-2-carbohydrazide (10 mmol) in 40 mL ethanol absolute, 2-hyroxy-4-methoxybenzaldehyde or salysaldehyde (10 mmole) was added. The reaction mixture was refluxed for 6hrs. The yellow solution was reduced in volume and allowed to slowly evaporate at room temperature. The obtained yellow solids were recrystalzied from ethanol to 1-3 in a good yield.

N'-(2-hydroxybenzylidene) pyrazine-2-carbohydrazide (hmbpcz) (1): Yellow solid. 1.79 g, 74% yield. Anal. Calc. for $C_{12}H_{10}N_4O_2$: C, 59.50; H, 4.16; N, 23.13; O, 13.21. Found: C, 59.55; H, 4.18; N, 23.20; O, 13.11%. IR (KBr, cm^{-1}) 3255 υ(O-H); 3192 υ(N-H); 3032 υ(=C-H); 2841 υ(C-H); 1672 υ(C=O); 1629 υ(C=N). ^{1}H NMR (DMSO-d_6, δ ppm): δ12.55 (*s*, H), 11.62 (*s*, H), δ9.27 (*s*, H), δ8.94 (*s*, H), δ8.80 (*s*, H), δ8.75 (*s*, H), 7.40 (*d*, J_{HH}= 8.00Hz, H); 6.53 (*d*, J_{HH}= 8.00Hz, H), δ6.51 (*s*, H), δ3.78 (*s*, 3H).

N'-(2-hydroxy-4-methoxybenzylidene) pyrazine-2-carbohydrazide (Hbpcz) (2)

Yellow solid. 2.1 g, 77% yield. Anal. Calc. for $C_{13}H_{12}N_4O_3$: C, 57.35; H, 4.44; N, 20.58; O, 17.63. Found: C, 57.33; H, 4.36; N, 20.60; O, 17.51%. IR (KBr, cm^{-1}) 3200 υ(O-H); 3190 υ(N-H); 3037 υ(=C-H); 2843 υ(C-H); 1691 υ(C=O); 1633 υ(C=N). ^{1}H NMR (DMSO-d_6, δ ppm): δ12.66 (*s*, H), 11.27 (*s*, H), δ9.29 (*s*, H), δ8.95 (*s*, H), δ8.86 (*s*, H), δ8.82 (*s*, H), 7.54 (*d*, J_{HH}= 8.00Hz, H); 7.34 (*d*, J_{HH}= 8.00Hz, H), δ6.95 (*s*, H).

N'-(2-hydroxy-4-methoxybenzylidene) benzohydrazide (Mbbz) (3)

Yellow solid. 1.88 g, 69% yield. Anal. Calc. for $C_{15}H_{14}N_2O_3$: C, 66.66; H, 5.22; N, 10.36; O, 17.76. Found: C, 66.71; H, 5.18; N, 10.40; O, 17.68%. IR (KBr, cm^{-1}) 3222 υ(O-H); 3182 υ(N-H); 3050 υ(=C-H); 2844 υ(C-H); 1680 υ(C=O); 1630 υ(C=N). ^{1}H NMR (DMSO-d_6, δ ppm): δ12.03 (*s*, H), 11.66 (*s*, H), δ8.56 (*s*, H), δ7.94 (*s*, H), δ7.62 (*s*, H), δ7.55 (*s*, H), 7.44 (*d*, 2H); 6.53 (*m*, 2H), δ3.79 (*s*, 3H).

Results and discussion

The synthesis of Hydrazone derivatives is illustrated in scheme 1 by following slightly adjusted literature method [15-17]. The synthesis is started by converting pyrazine-2-carboxylic acid into acid hydrazide via esterification. Then, the targeted compounds (1-3) were synthesized by simply mixing an equimolar amount of 4-methoxy-2-hydroxybenzaldehyde or salicaldehyde and carbohydrazide (Scheme 1). The resulting solution was left for slow evaporation, which gave yellow powder in an excellent yield.

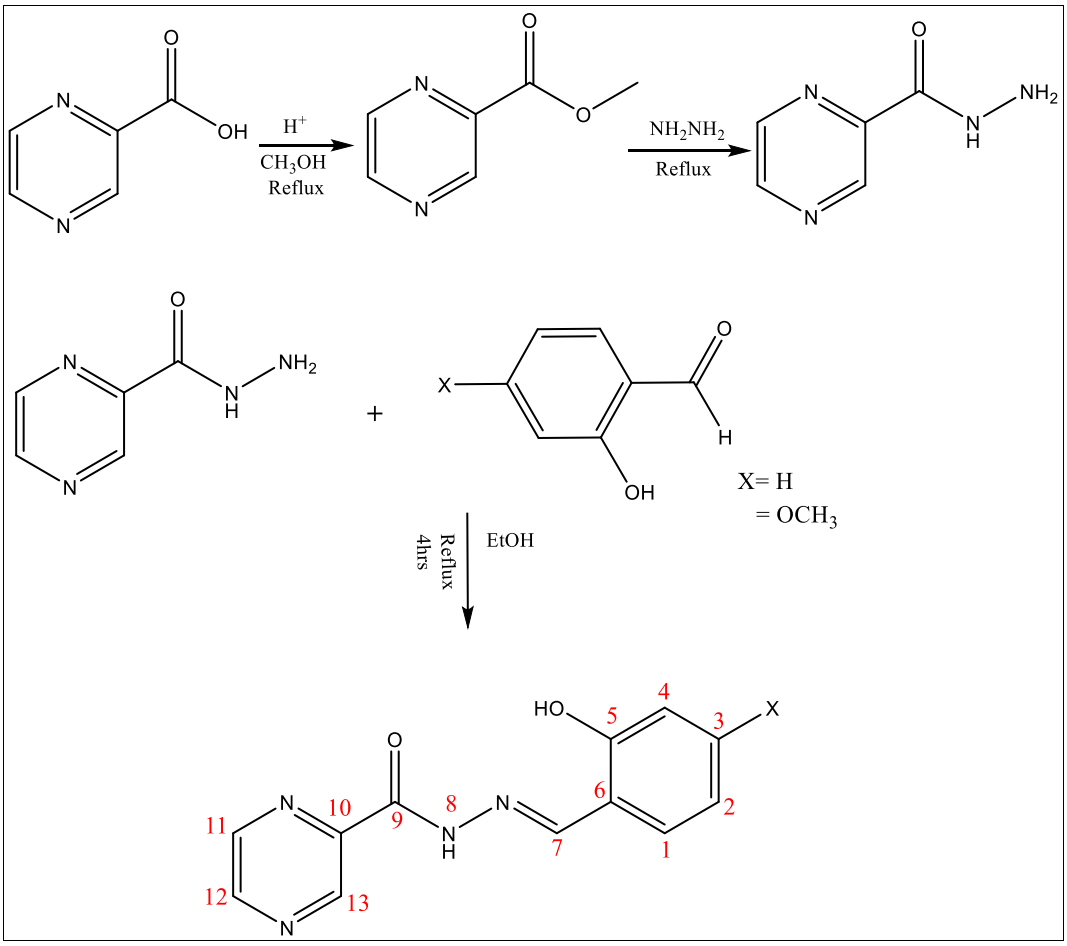

Scheme 1: Synthesis of carbohydrazide Schiff base derivatives

The IR and NMR data supported the formation of hydrazones derivatives. The hydrazones derivatives are soluble in most organic solvents and they are stable at room temperature.

IR Spectra

The IR spectra of the synthesized hydrazone derivatives (see supplementary files) showed the two distinctive groups υ(O-H) and υ(N-H) absorption band at 3255-3180 cm^{-1}. Also, the υ(=C-H) Aromatic absorption band appeared at 3037 cm^{-1}. The aliphatic υ(C-H) showed at 2841 cm^{-1}. While the carbonyl absorption band showed at 1690-1672 cm^{-1}. Finally, The Azomethane absorption band showed at 1633-1629 cm^{-1}.

Table 1: IR data of the synthesized complexes in (cm^{-1})

Compounds	υ(O-H)	υ(N-H)	υ(C-H)Ar	υ(C-H) aliphatic	υ(C=O)	υ(C=N)
Hmbpcz [1]	3255	3192	3032	2841	1672	1629
Hbpcz [2]	3200	3190	3037	----	1691	1633
Mbbz [3]	3222	3182	3050	2844	1680	1630

^{1}H-NMR Spectra

The ^{1}H-NMR chart of the synthesized hydrazone derivatives showed the presence of the amide proton at 12.55 ppm (s, 1H). While the proton of the phenolic group appeared at 11.62 pm (s, 1H). The distinctive Azomethane proton showed at 9.27 ppm (s, 1H). Moreover, the pyrazine ring showed three distinctive signals which displayed at 8.94 ppm (s, 1H), 8.80 ppm (s, 1H), and 8.75 ppm (s, 1H) corresponding the proton coded H13, H12, and H11 respectively. Furthermore, the benzene ring protons showed as following; a doublet at 7.40 ppm (d, 1H) which attributed to H1. A doublet at 6.54 ppm (d, 1H) which corresponds to H2. A singlet at 6.51 ppm (s, 1H) corresponding to H4. Finally, the methoxy group appeared as a singlet at 3.78 ppm (s, 3H).

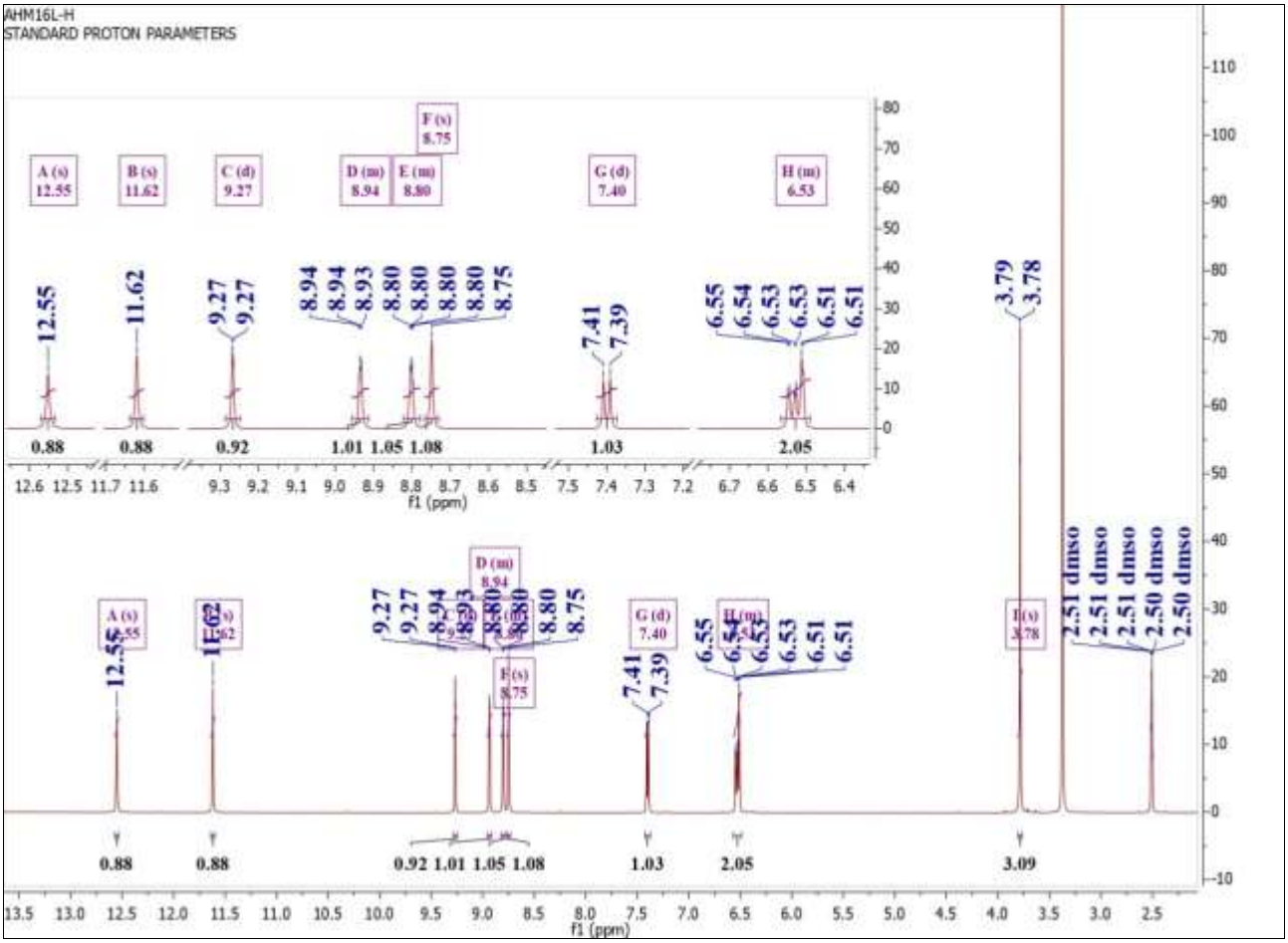

Fig 1: The ^{1}H-nmr chart for hmbpcz.

DFT Analysis

Computational Detail

Optimization, frequency calculation and electrostatic potential evaluation were done by Gaussian 09 program [18]. The level of B3LYP/Def2-TZVP (Triple zeta + polarization) was used for all self-consistence field (SCF) calculations. To start the calculations, the geometrical structures of the ligands were fully optimized by minimizing the forces on all atoms. In addition, the frequencies of all ligands were calculated by the second derivative of the energies to the coordinates to be sure that the geometries are in the local minima instead of saddle points. Since all frequencies are positive, the geometries are in the local minima. Important electron donor and acceptor orbitals and the values of the inter-orbital charge transfers were done by NBO 6.0 program [19]. The iso-surface density value was set to 0.02 e/$Å^3$ for drawing the graphical representation of molecular orbitals and electrostatic potential, and Gauss View program [20], was used to show the contour plots.

Computational studies

Geometrical and Electronic Properties

Fig. 2 shows the optimized structures of the ligands in the local minima. All the ligands are planar with a good π-electron resonance throughout the whole of the molecule.

Tables 2-4 show the bond lengths and angles for the optimized gas phase and the experimental solid phase. In all these tables, the root mean square deviation (RMSD) of bond lengths and bond angles are less than 0.02Å and 4°, respectively. These data show that the outputs of theoretical calculations are reliable.

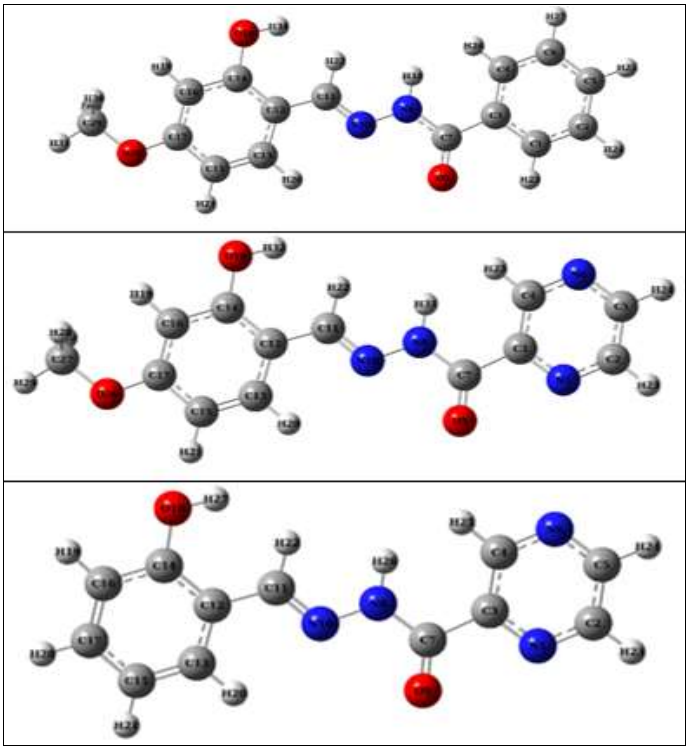

Fig 2. Optimized structure of the compounds 3 (up), 1 (middle), and 2 (down) optimized at the level of B3LYP/Def2-TZVP.

Fig. 3 shows the graphical representation of the highest occupied molecular orbital (HOMO) and the lowest unoccupied molecular orbital (LUMO) for the hydrazone derivatives. The LUMO is distributed throughout the entire molecule for all compounds, while the pyrazine ring does not contribute to the HOMO. The HOMO-LUMO gap is the highest value for the compound 3 and it is the lowest for the compound 1. It seems that the pyrazine group reduces the gap. The ligands with pyrazine group have both HOMO and LUMO with lower energies. On the other hand, CH_3O– group increases the energy levels of HOMO and LUMO. The atomic charges of all atoms have been presented in Tables S4-S6. These charges calculated by Multiwfn code [21] according to the Bader algorithm of Quantum theory of atoms-in-molecules (QTAIM) [22]. Both nitrogen atoms (N1 and N6) in the pyrazine groups of the compound 1 and 2 have higher charges compared to the carbon atoms (C1 and C6) in the compound 3. N1 atom has -1.098 and -1.103 *e* charge, and N6 has -1.140 and -1.127 *e* charge for compounds 1 and 2, respectively, while C1 atom has -0.022 *e* and C6 has -0.05 *e* charge. Both nitrogen atoms (N8 and N10) in the azo group have higher charges in the compounds 1 and 2 compared to the compound 1. The QTAIM charge of N8 in ligands 3, 1, and 2 is equal to -1.024, -1.035, and -1.034 *e*, respectively, while the charge of N10 is equal to -0.697, -0.701, and -0.704 *e*, respectively. The carbonyl carbon's charge is equal to +1.687, +1.715, and +1.719 *e* for compounds 3, 1, and 2, respectively. Fig. 4 shows the electrostatic potential (ESP) for three studied compounds. The ESP shows that the oxygen of carbonyl group has the highest minus ESP, and it is the best center for nucleophilic reaction, while hydrogens of OH and NH are the positive ESP center, and proper for the electrophilic reactions.

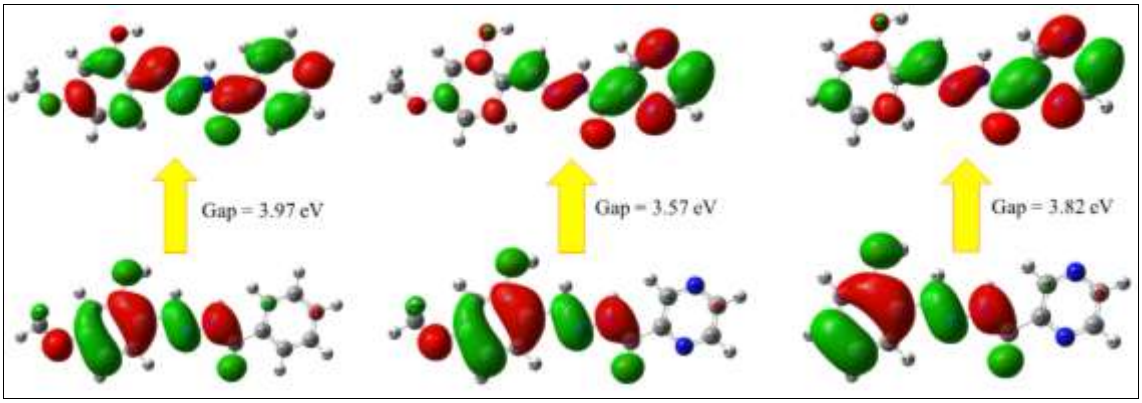

Fig 3: HOMO and LUMO for the studied compounds: left: compound 3, middle: compound 1, and right: compound 2.

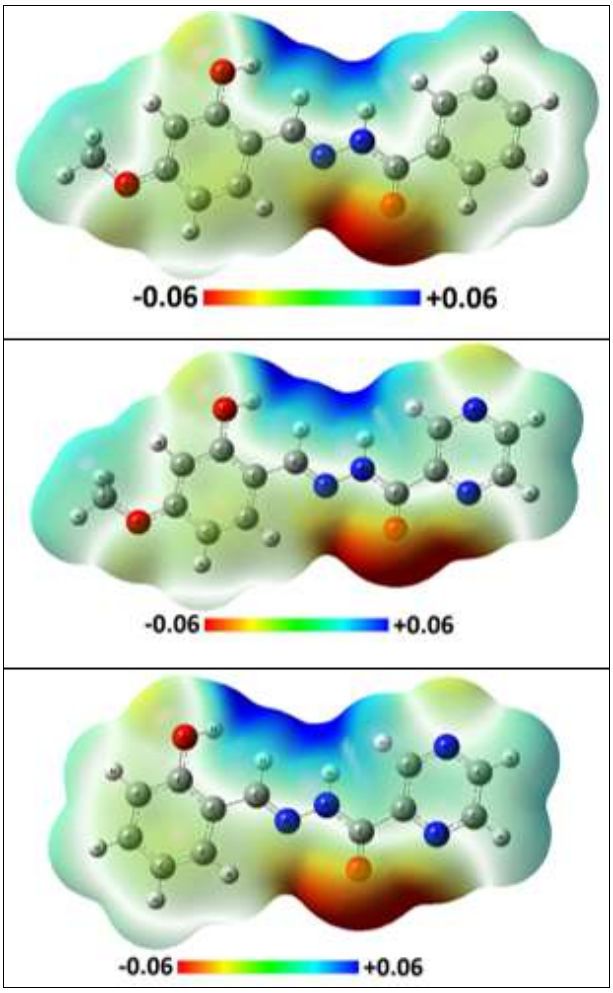

Fig 4: Electrostatic potential (ESP) calculated at the level of B3LYP/Def2-TZVP for compounds 3 (up), 1 (middle), and 2 (down) at the iso-surface density value of 0.02 e/A^3

NBO Analysis

The natural bond orbital (NBO) calculations were done to obtain electronic information about π-electron resonances in the pyrazine/benzene ring, azo/carbonyl group, and CN bond. Only cases are reported that their second order stabilization energies are more or equal to 15 kcal/mol ($E^{(2)}$≥15).NBO shows that all the ligands are planar due to the π-electron resonance throughout all the molecules. Aligned with the QTAIM charges, N1 and N6 in pyrazine ring have higher $E^{(2)}$ when they are electron donors. The higher charge density on these atoms help to donate better their electrons (compare, for example, $E^{(2)}$ for π_{N1-C2} to other π^* with the$E^{(2)}$ forπ_{C1-C2} to other π^*). On the other hand, the stabilization energy when they act as a role of an electron acceptor is less than the $E^{(2)}$ when carbon atom replaces nitrogen. N8 compared to N10 has higher QTAIM charge in all ligands, and NBO shows that as an electron donor, N8 has high stabilization energy ($E^{(2)}$> 30 kcal/mol). On the other hand, NBO shows that N10 can act as a good electron acceptor. In summary, NBO shows that all the ligands have high stabilization energies due to the π-electron resonance throughout the ligands. The highest π-electron resonance belongs to the lone pair of N8 as an electron donor and carbonyl π^* as an electron acceptor which stabilized the aromaticity by more than 50 kcal/mol.

Table 2: Stabilization energies (second order perturbation energies in kcal/mol) for donor-electron charge transfer in the compound 3.[1]

Donor	type	Acceptor	Type	$E^{(2)}$
$(LP1)_{N8}$	100% (p)	$(\pi^*)_{C7-O9}$	69% $(p)_{C7}$+31% $(p)_{O9}$	55.2
$(LP1)_{N8}$	100% (p)	$(\pi^*)_{N10-C11}$	44% $(p)_{N10}$+56% $(p)_{C11}$	32.0
$(LP2)_{O9}$	100% (p)	$(\sigma^*)_{C7-N8}$	62% $(sp^{2.3})_{C7}$+38% $(sp^{1.7})_{N8}$	30.6
$(LP2)_{O9}$	100% (p)	$(\sigma^*)_{C3-C7}$	49% $(sp^{2.4})_{C3}$+51% $(sp^{1.9})_{C7}$	22.6
$(\pi)_{C1-C2}$	48% $(p)_{C1}$+52% $(p)_{C2}$	$(\pi^*)_{C5-C6}$	51% $(p)_{C5}$+49% $(p)_{C6}$	21.9
$(\pi)_{C5-C6}$	49% $(p)_{C5}$+51% $(p)_{C6}$	$(\pi^*)_{C3-C4}$	49% $(p)_{C3}$+51% $(p)_{C4}$	21.6
$(\pi)_{C1-C2}$	48% $(p)_{C1}$+52% $(p)_{C2}$	$(\pi^*)_{C3-C4}$	49% $(p)_{C3}$+51% $(p)_{C4}$	20.4
$(\pi)_{C3-C4}$	51% $(p)_{C3}$+49% $(p)_{C4}$	$(\pi^*)_{C1-C2}$	52% $(p)_{C1}$+48% $(p)_{C2}$	19.6
$(\pi)_{C3-C4}$	51% $(p)_{C3}$+49% $(p)_{C4}$	$(\pi^*)_{C5-C6}$	51% $(p)_{C5}$+49% $(p)_{C6}$	19.3
$(\pi)_{C5-C6}$	49% $(p)_{C5}$+51% $(p)_{C6}$	$(\pi^*)_{C1-C2}$	52% $(p)_{C1}$+48% $(p)_{C2}$	18.6
$(\pi)_{C3-C4}$	51% $(p)_{C3}$+49% $(p)_{C4}$	$(\pi^*)_{C7-O9}$	69% $(p)_{C7}$+31% $(p)_{O9}$	18.0

[1]LP means lone pair. Only energies greater than 15 kcal.mol^{-1} were considered. Rydberg (very high energy) orbitals were not considered.

Table 3: Stabilization energies (Second order perturbation energies in kcal/mol) for donor-electron charge transfer in the compound 1 and 2.[1]

Donor	type	Acceptor	type	$E^{(2)}$
$(LP1)_{N8}$	100% (*p*)	$(\pi^*)_{C7-O9}$	68% $(p)_{C7}$+32% $(p)_{O9}$	53.9
$(LP1)_{N8}$	100% (*p*)	$(\pi^*)_{N10-C11}$	44% $(p)_{N10}$+56% $(p)_{C11}$	30.9
$(LP2)_{O9}$	100% (*p*)	$(\sigma^*)_{C7-N8}$	62% $(sp^{2.3})_{C7}$+38% $(sp^{1.7})_{N8}$	31.5
$(LP2)_{O9}$	100% (*p*)	$(\sigma^*)_{C3-C7}$	48% $(sp^{2.3})_{C3}$+52% $(sp^{2})_{C7}$	26.7
$(\pi)_{C5-N6}$	43% $(p)_{C5}$+57% $(p)_{N6}$	$(\pi^*)_{C3-C4}$	49% $(p)_{C3}$+51% $(p)_{C4}$	24.8
$(\pi)_{N1-C2}$	56% $(p)_{N1}$+44% $(p)_{C2}$	$(\pi^*)_{C3-C4}$	49% $(p)_{C3}$+51% $(p)_{C4}$	24.3
$(\pi)_{C3-C4}$	51% $(p)_{C3}$+49% $(p)_{C4}$	$(\pi^*)_{N1-C2}$	44% $(p)_{N1}$+56% $(p)_{C2}$	20.3
$(\pi)_{C3-C4}$	51% $(p)_{C3}$+49% $(p)_{C4}$	$(\pi^*)_{C5-N6}$	57% $(p)_{C5}$+43% $(p)_{N6}$	19.8
$(\pi)_{N1-C2}$	56% $(p)_{N1}$+44% $(p)_{C2}$	$(\pi^*)_{C5-N6}$	57% $(p)_{C5}$+43% $(p)_{N6}$	18.8
$(\pi)_{C5-N6}$	43% $(p)_{C5}$+57% $(p)_{N6}$	$(\pi^*)_{N1-C2}$	44% $(p)_{N1}$+56% $(p)_{C2}$	17.2
$(\pi)_{C3-C4}$	51% $(p)_{C3}$+49% $(p)_{C4}$	$(\pi^*)_{C7-O9}$	68% $(p)_{C7}$+32% $(p)_{O9}$	15.0

[1]LP means lone pair. Only energies greater than 15 kcal.mol^{-1} were considered. Rydberg (very high energy) orbitals were not considered. The selected data for both the compounds 1 and 2 are the same, only the atomic labels are different.

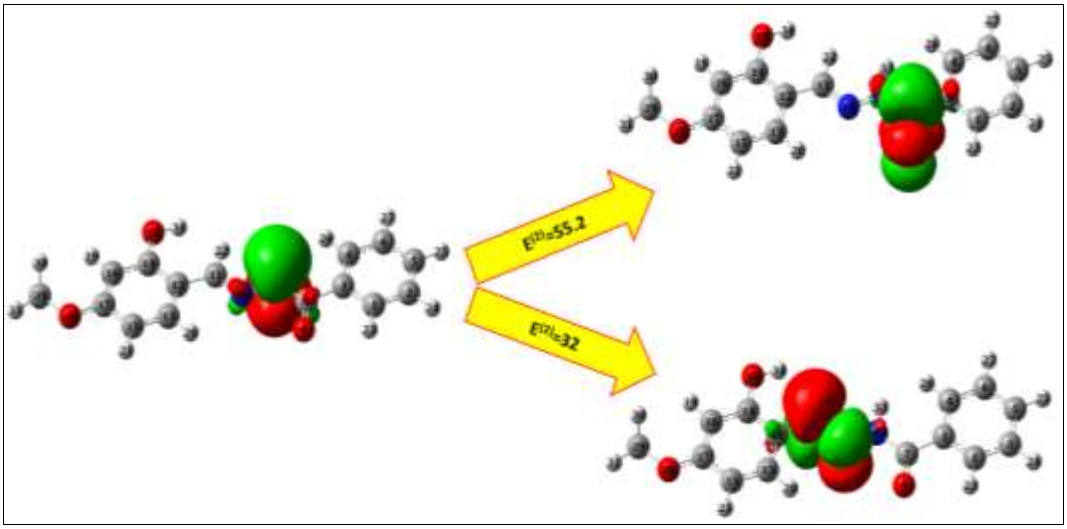

Fig 5: Donor (LPN8) and acceptors ($(\pi^*)_{C7-O9}$ and $(\pi^*)_{N10-C11}$) orbitals with the highest $E^{(2)}$ for the compound **3**. All units of $E^{(2)}$ are in kcal mol^{-1}. See the Table 1 for more detailed information.

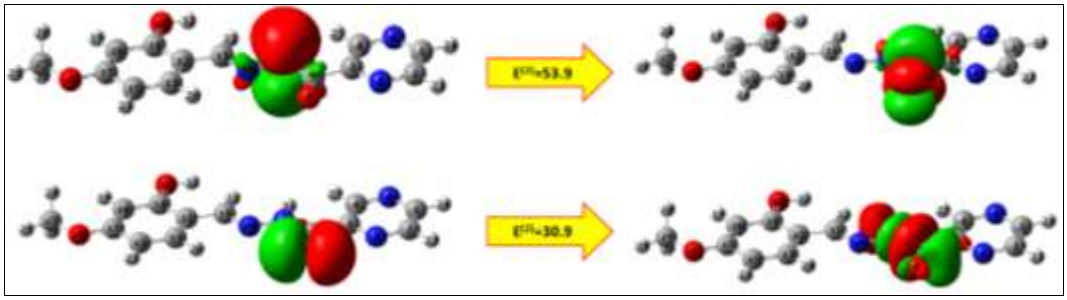

Fig 6: Donors (LPN8 and LP O9) and acceptors ($(\pi^*)_{C7-O9}$ and $(\pi^*)_{N10-C11}$) orbitals with the highest $E^{(2)}$ for the compounds 1 and 2. All units of $E^{(2)}$ are in kcal mol^{-1}. See the Table 2 for more detailed information.

Conclusion

Upon treating pyrazine-2-methanoate with hydrazine hydrate, pyrazine carbohydrazide were obtained. The pyrazine carbohydrazide were further reacted with suitable aldehydes in 1:1 molar ratio to afford the carbohydrazide derivatives; N'-(2-hydroxybenzylidene)pyrazine-2-carbohydrazide (Hmbpcz), N'-(2-hydroxy-4-methoxybenzylidene)pyrazine-2-carbohydrazide (Hbpcz), and N'-(2-hydroxy-4-methoxybenzylidene)benzohydrazide (Mbbz). Structural determination of these compounds was achieved using IR and NMR techniques, followed by theoretical investigation. The density functional theory (DFT) investigation revealed that the three compounds have a planar shape characterised by a high π-electron resonance. It is hypothesised that the nitrogen atoms in the pyrazine ring reduce the energy gap between the highest occupied molecular orbital (HOMO) and lowest unoccupied molecular orbital (LUMO) and enhance the stability of the molecule relative to aromatic non-nitrogen compounds.

Acknowledgements

The authors are thankful to Tikrit University, and Ardakan University for supporting this work.

Conflict of interest

The authors declare that they have no known competing financial interests or personal relationships that could have appeared to influence the work reported in this paper.

Author Contributions

Thaaer Khalil, Khalaf A. Jasim and Ahmed S. Faihan conducted the experiment, Reza Behjatmanesh-Ardakani

conducted the DFT calculations, Ahmed S. Faihan and Ahmed S. Al-Janabi wrote and revised the manuscript. All authors agreed to the final version of this manuscript.

References

1. Neumann DM, Cammarata A, Backes G, Palmer GE, Jursic BS. Synthesis and antifungal activity of substituted 2,4,6-pyrimidinetrione carbaldehyde hydrazones. Bioorg Med Chem. 2014;22:813.
2. Tapanyigit O, Demirkol O, Guler E, Ersatur M, Cam ME, Giray ES. Synthesis and investigation of anti-inflammatory and anticonvulsant activities of novel coumarin-diacylated hydrazide derivatives. Arab J Chem. 2020;13:9105-17.
3. Gihsoy A, Terzioglu N, Otuk G. Synthesis of some new hydrazide-hydrazones, thiosemicarbazides, and thiazolidinones as possible antimicrobials. Eur J Med Chem. 1997;32:753.
4. Rollas S, Gulerman N, Erdeniz H. Synthesis and antimicrobial activity of some new hydrazones of 4-fluorobenzoic acid hydrazide and 3-acetyl-2,5-disubstituted-1,3,4-oxadiazolines. Farmaco. 2002;57:171.
5. Yousef TA, Al-Jibori LHK, Fiahan AS, Elzupir AO, Abou-Krisha MM, Al-Janabi ASM. Benzohydrazide derivative metal complexes: Antimicrobial and inhibitory effects on liver cancer cell lines and quinone oxidoreductase 2-Experimental, molecular docking, and DFT investigations. J Mol Struct. 2024;1308:138073.
6. Kumar M, Roy S, Faizi MSH, Kumar S, Singh MM, Kishor S, *et al.* Synthesis, crystal structure, and luminescence properties of acenaphthene benzohydrazide-based ligand and its zinc(II) complex. J Mol Struct. 2017;1128:195-204.
7. Tabernero V, Cuenca T, Herdtweck E. Hydrazonide titanium derivatives: Synthesis, characterization, and catalytic activity in olefin polymerization. J Organomet Chem. 2002;663:173-182.
8. Zhong X, Wei HL, Liu WS, Wang DQ, Wang X. The crystal structures of copper (II), manganese(II), and nickel(II) complexes of a (Z)-2-hydroxy-N′-(2-oxoindolin-3-ylidene)benzohydrazide-Potential antitumor agents. Bioorg Med Chem Lett. 2017;17:3774-7.
9. Choudhary S, Morrow JR. Dynamic acylhydrazone metal ion complex libraries: A mixed-ligand approach to increased selectivity in extraction. Angew Chem Int Ed. 2002;41:4096.
10. Backes GL, Neumann DM, Jursic BS. Synthesis and antifungal activity of substituted salicylaldehyde hydrazones, hydrazides, and sulfohydrazides. Bioorg Med Chem. 2014;22:4629-4636.
11. Pelttari E, Karhumaki E, Langshaw J, Elo H. Carbohydrazones of substituted salicylaldehydes as potential lead compounds for the development of narrow-spectrum antimicrobials. Z Naturforsch C. 2014;62:483-486.
12. Pelttari E, Karhumaki E, Langshaw J, Perakyla H, Elo H. Antimicrobial properties of substituted salicylaldehydes and related compounds. Z Naturforsch C. 2014;62:487-497.
13. Shi L, Ge H, Tan S, Li H, Song Y, Zhu H, *et al.* Synthesis and antimicrobial activities of Schiff bases derived from 5-chloro-salicylaldehyde. Eur J Med Chem. 2007;42(4):558-564.
14. The B Alliance. Tuberculosis. 2008;88:141-144.
15. Abdel-Aziz M, Abdel-Rehman HM. Synthesis and anti-mycobacterial evaluation of some pyrazine-2-carboxylic acid hydrazide derivatives. Eur J Med Chem. 2010;45:3384-3388.
16. Majumdar P, Pati A, Patra M, Behera RK, Behera AK. Acid hydrazides: Potent reagents for synthesis of oxygen-, nitrogen-, and/or sulfur-containing heterocyclic rings. Chem Rev. 2014;114(5):2942-2977.
17. Goodman A, McCall JR, Jacocks HM, Thompson A, Baden D, Abraham WM, *et al.* Structure-activity relationship of brevenal hydrazide derivatives. Mar Drugs. 2014;12:1839-1858.
18. Frisch MJ, Trucks GW, Schlegel HB, Scuseria GE, Robb MA, Cheeseman JR, *et al.* Gaussian 09, Revision E.01. Wallingford, CT; c2009.
19. Glendening ED, Landis CR, Weinhold F. NBO 6.0: Natural bond orbital analysis program. J Comput Chem. 2013;34:1429-1437.
20. Dennington R, Keith TA, Millam JM. GaussView, Version 5.0. Shawnee Mission, KS: Semichem Inc.; c2016.
21. Lu T, Chen F. Multiwfn: A multifunctional wavefunction analyzer. J Comput Chem. 2012;33:580-592.
22. Bader RFW. Atoms in molecules: A quantum theory. Oxford: Clarendon Press; c1994.